AIP | Review of Scientific Instruments

New ultrarapid-scanning interferometer for FT-IR spectroscopy with microsecond time-resolution

B. Süss, F. Ringleb, and J. Heberle

Citation: Review of Scientific Instruments **87**, 063113 (2016); doi: 10.1063/1.4953658

View online: http://dx.doi.org/10.1063/1.4953658

View Table of Contents: http://scitation.aip.org/content/aip/journal/rsi/87/6?ver=pdfcov

Published by the AIP Publishing

New ultrarapid-scanning interferometer for FT-IR spectroscopy with microsecond time-resolution

B. Süss,[1] F. Ringleb,[2,a)] and J. Heberle[1,b)]
[1]*Department of Physics, Experimental Molecular Biophysics, Freie Universität Berlin, Arnimallee 14, 14195 Berlin, Germany*
[2]*Institute for Crystal Growth, Max-Born Straße 2, 12489 Berlin, Germany*

(Received 15 March 2016; accepted 30 May 2016; published online 15 June 2016)

A novel Fourier-transform infrared (FT-IR) rapid-scan spectrometer has been developed (patent pending EP14194520.4) which yields 1000 times higher time resolution as compared to conventional rapid-scanning spectrometers. The central element to achieve faster scanning rates is based on a sonotrode whose front face represents the movable mirror of the interferometer. A prototype spectrometer with a time resolution of 13 μs was realized, capable of fully automated long-term measurements with a flow cell for liquid samples, here a photosynthetic membrane protein in solution. The performance of this novel spectrometer is demonstrated by recording the photoreaction of bacteriorhodopsin initiated by a short laser pulse that is synchronized to the data recording. The resulting data are critically compared to those obtained by step-scan spectroscopy and demonstrate the relevance of performing experiments on proteins in solution. The spectrometer allows for future investigations of fast, non-repetitive processes, whose investigation is challenging to step-scan FT-IR spectroscopy. *Published by AIP Publishing.* [http://dx.doi.org/10.1063/1.4953658]

I. INTRODUCTION

Infrared absorption spectroscopy is an analytical tool to identify molecules and molecular changes by their characteristic vibrational spectrum. With the advent of Fourier-transform infrared (FT-IR) spectroscopy which was commercialized in the late 1960s, broadband spectral information is recorded within fractions of a second at high spectral resolution. In combination with a high time resolution, tracing reactions, rapid process monitoring or remote sensing and identification can be realized. The commercially available rapid-scan technology is limited to about 100 scans/s basically due to the moment of inertia of the movable mirror. A faster type of rapid-scan spectrometers, presented by Manning, *et al.*, are rotating spectrometers which are able to achieve about 1000 scans/s.[1,2] In conclusion, the temporal resolution of rapid-scan spectrophotometry is limited to 10 ms – 1 ms. These limitations of the conventional rapid-scan technique are circumvented by the application of the step-scan approach. Here, each retardation point of the interferogram is recorded. As often thousands of identical samples in a perfectly stable environment are required for step-scan recordings, this method is hardly applicable to irreversible reactions. The same limitations hold for stroboscopic interferometry and asynchronous sampling.[3] Photoacoustic spectrometry (PA) is a valuable tool for the investigation of surfaces, thin films, and opaque samples. However, because the thermal diffusion depth varies with the square root of the modulation frequency of the incident radiation (i.e., the velocity of the moving mirror), the layer thickness to be probed is limited by the moving mirror of the spectrometer. Since the penetration depth is a function of the mirror frequency multiplied by the specific wavenumber, a variation in penetration depth is present in the spectrum.[4] To circumvent this problem, modulated step scan PA can be applied.[5]

Another novel method of IR spectroscopy is the use of tunable quantum cascade lasers (QCLs). Those lasers emit strong IR intensities and allow measurements with non-repetitive samples since the condition *sine qua non* of perfect reproducibility of the reaction is not as mandatory as with the step-scan technology. The drawback of QCLs is that each wavenumber has to be measured separately and multiple measurements are necessary to cover a certain spectral range. Moreover, the tunability of QCLs is currently limited to 200 cm^{-1} (in cw operation).[6] Thus, the purchase of many QCL heads is required to cover the spectral range of FT-IR spectrometers which is not cost-effective.

Here, a new approach for ultrarapid-scanning FT-IR spectrometry is introduced that yields unprecedented temporal resolution while retaining broad spectral coverage at a single measurement. Time-resolved FT-IR experiments will be presented that were recorded with a prototype device based on the new interferometer design. The membrane protein bacteriorhodopsin (bR) was chosen as a model system to trace protein reactions because bR is robust and due to the reversibility of the process amenable to the step-scan technique[7] which is the critical reference technique herein.[8,9] Light-induced FT-IR difference spectroscopy[10] is applied to resolve the structural and chemical changes that render bR a proton pump.[11,12] High quality light-induced difference spectra have been obtained at a time resolution of 13 μs. Moreover, the high fidelity of the data render the technique applicable to proteins dissolved in excess solvent. Difference spectra of bR suspended in excess D_2O and probed in a flow-cell are recorded with excellent

a)This research was performed while F. Ringleb was at Fritz Haber Institute of the Max Planck Society, Berlin 14195, Germany.
b)Electronic mail: joachim.heberle@fu-berlin.de.

signal-to-noise ratio (SNR) to determine structural alteration as minute as protonation and hydrogen-bonding changes on the level of single amino acid side chains. It will be shown that peptide backbone changes of the dissolved protein are larger as compared to the protein film immersed in solution as used with ATR sampling.

II. INSTRUMENT DESCRIPTION

A. General principle

A major obstacle for increasing the time resolution in rapid-scanning FT-IR spectroscopy is to create a sufficient optical path length difference (OPD) in a very short period of time. This path length difference is reciprocally related to the resolution, e.g., 1 cm for 1 wavenumber resolution. To create the desired OPD, which oscillates around zero, a moving mirror is usually accelerated and deaccelerated rapidly. A limited maximum force and power make it impossible to realize a time resolution better than in the lower ms range.[13] The fundamental idea of the presented invention is to use a mechanical resonator as source for generating the OPD.

The surface of an ultrasonic resonator can be employed as a mirror oscillating at high amplitudes and velocities, to exceed any parameters achieved so far by conventional traveling mirrors. The resonator material must be of tough quality such as steel or titanium, to withstand the strong stress occurring during operation. An ultrasonic acoustic wave is generated by a piezo-oscillator and fed into the resonator (Figure 1). The design of the resonator leads to a strong amplification of the oscillation amplitude.[14,15] Mounting a mirror to the resonator disturbs the resonant frequency and even worse, the time resolution is degraded dramatically. For this reason, the moving mirror is realized as a polished/lapped surface of the resonator with a thin gold coating as reflecting surface with a diameter of 18 mm. The IR beam is reflected four times at two distinct positions on the sonotrode's surface. The presented spectrometer comprises a 19.2 kHz resonator allowing a maximal time resolution of 13 μs, which corresponds to 76 923 scans/s. This is achieved by recording double-sided interferograms (two per oscillation) and subsequent splitting of the interferograms. The oscillating frequency and amplitude of the sonotrode is limited by the material properties and in the present case at around 270 μm (peak to peak) at the surface of the sonotrode. The amplitude of the converter is amplified by a factor of 10.5 with the help of booster and sonotrode. Due to the OPD amplification of a factor of 4 (optical path with four reflections on the sonotrode, see Fig. 2), the maximal spectral resolution is 9 cm^{-1}, which can be increased to 5 cm^{-1} in single-sided operational mode (at a time resolution of ~26 μs). In single-sided mode, the interferogram peak is shifted from the middle of the sonotrode amplitude to one of the turning points by the displacement of the static mirror. Even though the spectrometer is capable of 9 cm^{-1} spectral resolution, the presented spectra have been recorded at 12 cm^{-1} resolution. By this procedure, the signal-to-noise ratio is optimized and the mechanical stress of the sonotrode is reduced under continuous operation for many hours (>15 h). A 500 W generator was used (UIP500hd, *Hielscher*) for ultrasonic excitation. Standard commercially available resonators were used as booster and sonotrode (*Hielscher*). The surface of the titanium sonotrode was lapped and galvanically gold coated to implement a mirrored surface.

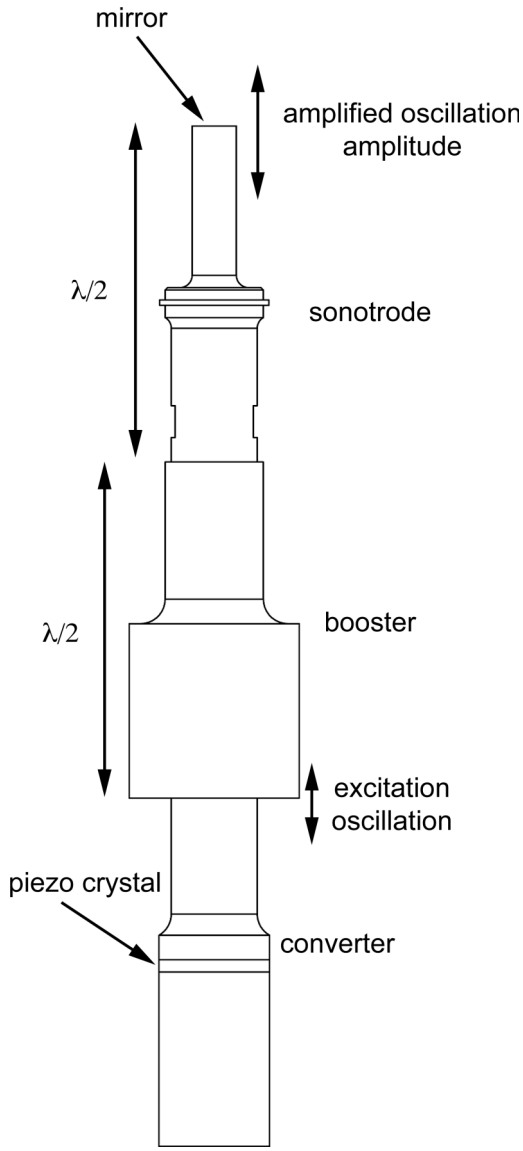

FIG. 1. Schematic representation of the ultrasonic resonator applied in the prototypic spectrometer presented here. The length of λ/2 refers to the wavelength of the soundwave inside the sonotrode. The ultrasonic wave is created by the piezo-crystal and led into the converter. The booster amplifies the oscillation amplitude and leads the acoustic wave into the sonotrode. The sonotrode amplifies the oscillation as well and finally the surface of the sonotrode is used as moving mirror of the spectrometer.

B. Experimental setup

An IR broadband globar is used (*NGK Glow Plug*) as light source. The emission is collimated by a silver-coated off-axis parabolic mirror with a reflected focal length of 101.6 mm. A combination of a coated and wedged CaF_2 substrate and a wedged CaF_2 compensator are used as beamsplitter. The static interferometer arm comprises a retroreflector to facilitate accurate OPD adjustment. To increase the OPD and to include shear and tilt compensation, a cube corner mirror setup like

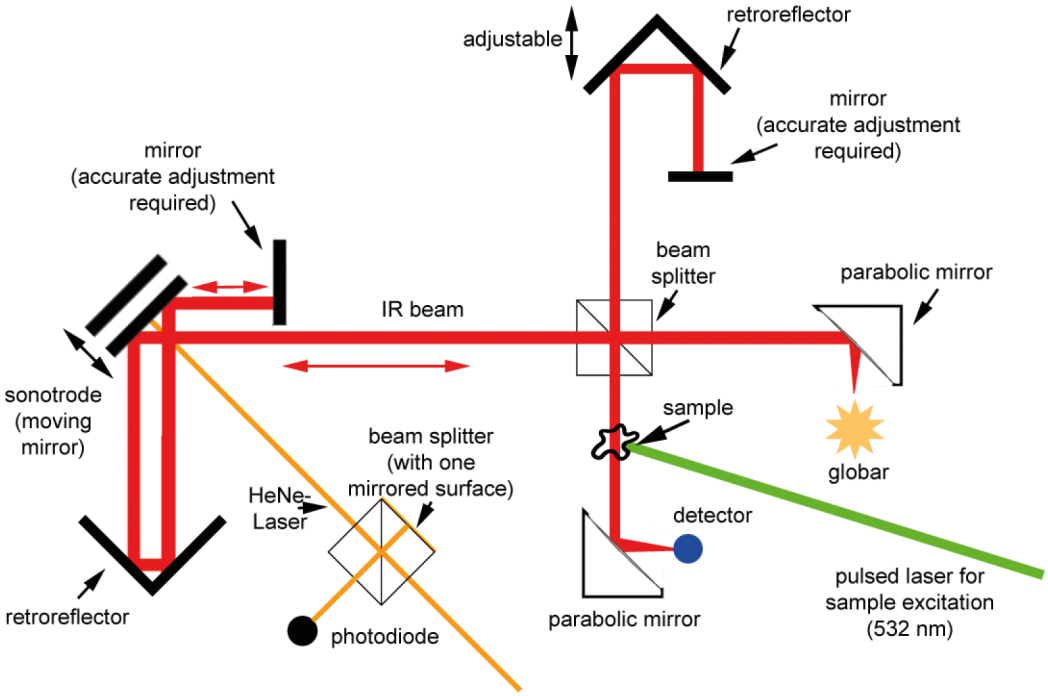

FIG. 2. Optical layout of the ultrarapid scanning FT-IR spectrometer comprising the sonotrode as a moving mirror and a retroreflector for increasing the OPD and compensating for tilt and sheer of the sonotrode (red line). A separate interferometer (yellow line) to determine the sonotrode position and an excitation laser (green line) for triggering photolytic reactions are also depicted.

in Ref. 2 is used. The four reflections on the moving mirror lead to an OPD amplification of a factor of four. The oscillation of the resonator is monitored by detecting the intensity of a HeNe laser in a separate interferometer. This is to minimize the sample frequency of the acquisition system as the OPD of the laser is not amplified. The HeNe signal is detected by a pin photodiode (*Thorlabs,* PDA10A). The IR signal is detected by a MCT detector (*Kolmar Technologies*, 50 MHz electrical bandwidth; 0.5 mm diameter) and amplified by a transimpedance amplifier (*Femto*, HCA-S; 40 MHz BW; 25 kV/A). The high bandwidths are crucial due to the high fringe frequencies of the individual IR frequencies at the interferogram centerburst, e.g., ~34.5 MHz for 2500 cm^{-1}. Both signals are recorded by a 200 MS/s 14 bit AD-Card (*GaGe Razor*). To account for small changes in the globar intensity or variations in the sample absorption, an automatic bias regulation for the MCT preamplifier is implemented to prevent saturation. As temperature variations can change the OPDs of the interferometer, an automatic adjustment of the static OPD is realized by moving the retroreflector on a servomotor controlled linear stage. Both adjustments are performed prior to the actual recording. In case of multiple measurements, a new automatic adjustment starts every tenth measurement.

C. Data evaluation

Unlike conventional spectrometers, a constant mirror velocity is neither achievable nor required. Instead, aiming for a constant velocity would reduce the duty cycle significantly. To circumvent this traditional approach and to gain equidistant sample points in OPD, the signal is measured by sampling equidistant in the time domain and applying a digital low pass filter to obtain the sampling points at the corresponding zero-crossings of the HeNe laser fringes.[16] The zero crossings are approximated by a linear interpolation of the data points. As the HeNe fringe frequency changes during a scan from 0 to >100 MHz (Figure 3), an adaptive digital low-pass filter ("sinc filter") for the IR data is realized by a convolution approach. The cutoff frequency of the low-pass filter at a distinct mirror position is determined by the actual mirror velocity, which is determined by the HeNe fringe frequency. This leads to an increase in signal-to-noise ratio at the edges of the interferogram, where the signal is significantly lower. An additional digital high-pass filter is used to eliminate DC components

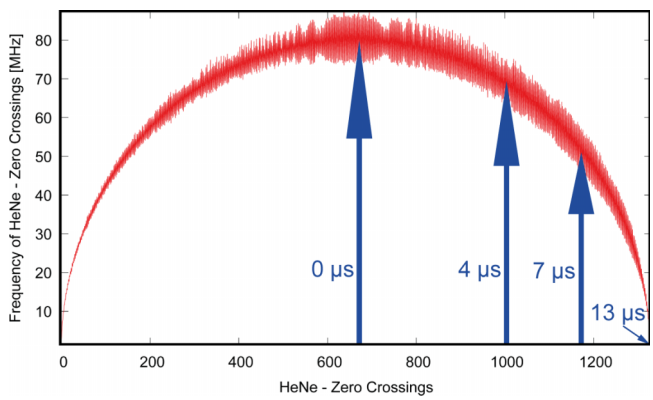

FIG. 3. Zero crossings of the HeNe laser intensity signal over the frequency of the occurrences of the zero crossings. The IR sample points are taken at the zero crossings to provide equidistant points in the OPD. Data were taken The spectral resolution is 12 cm^{-1}. A triggered measurement is started at the interferogram centerburst (see blue arrow at 0 μs). Due to the varying mirror velocity, half the OPD (corresponding to the spectral resolution of 24 cm^{-1}) is reached after 4 μs, three quarters of the resolution is reached at 7 μs, and full resolution at 13 μs.

and low-frequency distortions. Finally, a digital Fast Fourier Transformation (FFT) of the interferogram results in the IR spectra.

D. Trigger

The time-resolved measurements are initiated by a nanosecond laser flash of the 2nd harmonic of a Nd:YAG laser (~5 ns pulse width; ~5 mJ/cm^2 energy density; 532 nm wavelength, *Continuum* model Minilite I). This excitation has to be precisely synchronized with the spectrometer to occur each time at the same position of the interferogram to ensure consistency in averaged data and a temporally defined first spectrum. As the resonator positon cannot be controlled at a distinct time, the spectrometer is master and the laser is slaved. This is achieved by monitoring the interferogram intensity and release of the trigger event at its centerburst position. As a consequence, the first interferogramm is only half sided and takes 13 μs. As the mirror velocity is strongly varying during the data acquisition (Figure 3), with the maximum of velocity at the interferogramm centerburst, this triggering method also facilitates the possibility to gain even higher time resolution for the first (and exclusively for the first) interferogram by truncation of the OPD. However, the improved temporal resolution is paid-off by a decrease in spectral resolution for the first interferogram. Half of the maximum resolution can already be acquired after 4 μs, and three quarters of the full resolution after 7 μs. This facilitates an insight to the fast events occurring at the early stages of the reaction.

E. Performance

For an initial estimate of the performance of the spectrometer, the theoretical signal-to-noise ratio (SNR) is compared to experimental data. A single interferogram with a retardation corresponding to a spectral resolution of 12 cm^{-1} results in a SNR of 1382 (Figure 4). This value based on the assumption that the signal corresponds to the peak-to-peak signal of the interferogram centerburst. The peak-to-peak signal variations of the outer limits of the interferogram were used as noise floor. The theoretical SNR is given by[17]

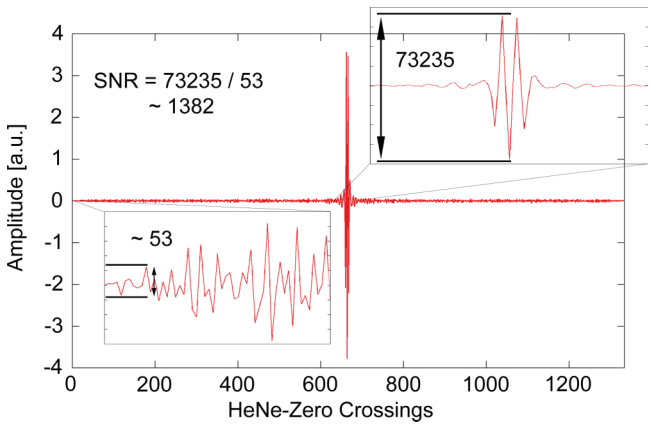

FIG. 4. Interferogram recorded with the prototype spectrometer showing the signal-to-noise ratio. The scan time for the double-sided interferogram was 26 μs at a spectral resolution of 12 cm^{-1}.

$$SNR = \frac{U_\nu(T)\,\theta\Delta\tilde{\nu}\sqrt{t}D^*\xi}{\sqrt{A_D}}. \quad (1)$$

The spectral brightness $U_\nu(T)$ is given by the Planck equation at a typical globar temperature of 1500 K. The optical throughput θ of the prototype spectrometer is derived by the multiplication of the solid angle of the IR beam being focused on the detector computed as shown in Ref. 18 (using a IR beam diameter of 8 mm and a focal length of 2.032 cm) with the detector area and is calculated to 0.232×10^{-3} cm^2·sr. A spectral resolution of $\Delta\nu = 12$ cm^{-1}, time resolution t of 26 μs (for a double-sided scan), detectivity of $D^* = 6.06 \times 10^{-10}$ Jones at 1 MHz, and a detector area $A_D = 1.96 \cdot 10^{-3}$ m^2 were used. Referring to Ref. 17, 0.1 is a common value for the efficiency factor ξ in commercial spectrometers. This leads to a theoretically achievable *SNR* of ~2720, which is about a factor of two more as compared to the experimental value (see above). Considering uncertainties in values like the globar temperature, the detectivity at higher modulation frequencies, and the light scattering due to the non-perfect sonotrode surface (caused by the difficult lapping process of the titanium), this value seems to be reasonable for this prototypic device and shows the good overall performance of the setup.

III. TIME-RESOLVED FT-IR DIFFERENCE EXPERIMENTS ON BACTERIORHODOPSIN

A. Data recording

Interferogram and HeNe data are recorded for 100 ms after laser excitation. The last 100 spectra are averaged and used as a background spectrum. The data set consists of 110 000 averaged experiments (comparable to ~70 step-scan experiments), i.e., 110 000 laser excitations with subsequent recordings of 3847 double-sided interferograms. So for each time point, 110 000 single spectra were averaged. For Figs. 5 and 6, a digital low-pass filter is applied in the time domain for spectra later than 100 μs. The cutoff frequency is chosen to satisfy Shannon's sampling theorem for the corresponding time decade (100 μs, 1 ms and 10 ms sampling steps). To provide a replicable and reproducible baseline correction, a digital high-pass approach similar to Ref. 19 is used to filter very low frequency distortions, but instead of a FFT a convolution approach was used. Absorbance changes at distinct wavenumbers are analyzed by sums of exponentials.

B. Sampling cell

To show the applicability to non-cyclic reactions, a sample in solution was chosen to facilitate measurements in a native environment and to provide an easy sample exchange. A flow-cell was constructed comprising a polyethylene (PE) spacer ring with a thickness of ~12 μm and an inner diameter of 10 mm, and two 2 mm thick channels lead to the in- and outlet. This spacer is placed between two CaF_2 windows leading to a sample volume of ~0.95 μl. In- and outlets are drilled into one CaF_2 window and microtubes are connected by fittings. The sample is exchanged by applying air pressure to a sample reservoir connected to the microtubes. The flow is controlled by two electromagnetic valves where one controls the pressure

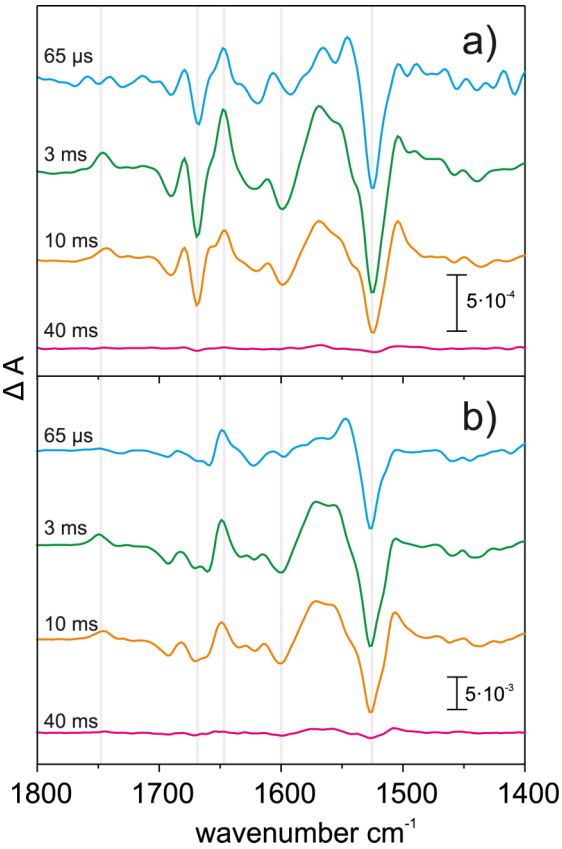

FIG. 5. Time-resolved FT-IR difference spectra of bacteriorhiodopsin (bR). Spectra at 65 μs, 3 ms, 10 ms, and 40 ms are shown after pulsed photonic excitation. (a) recorded with the ultrarapid-scanning spectrometer on purple membranes suspended in D_2O at a concentration of 15 mg/ml (pD 7, 150 mM KCl). (b) Corresponding difference spectra recorded on a film of bR recorded with the step-scan technique. The bR film was dried on a ZnS prism and immersed in a solution of 1 M KCl, pD 6.6. Experiments were performed using the ATR technique (see Ref. 9 for more details).

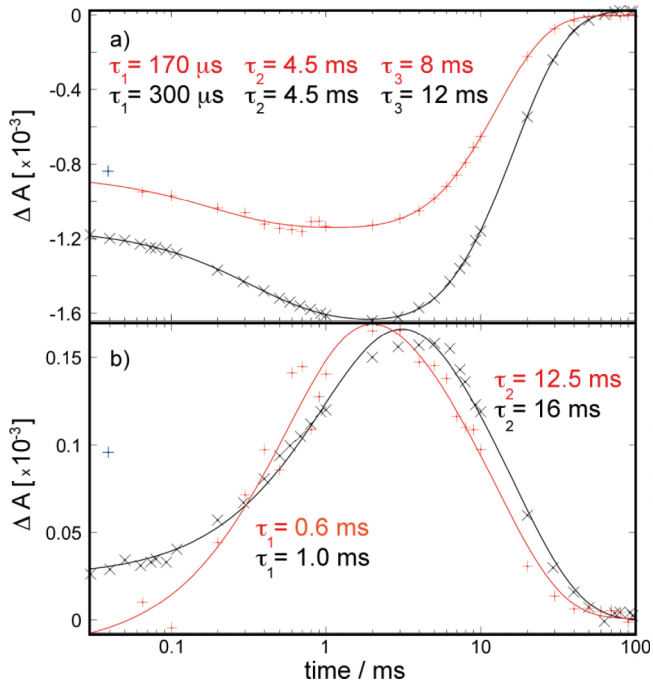

FIG. 6. (a) Kinetics of the band at 1526 cm^{-1} (red x) of bR in solution and recorded by the ultrarapid-scan technique as compared to bR recorded by the step-scan ATR technique (black +). The absorption changes of the latter data have been divided by a factor of 10 to facilitate the direct comparison. The continuous lines correspond to 3-exponential fits to the data. (b) Kinetics at 1746 cm^{-1} corresponding to deuteron transfer to D85.

and a second vents the tubes for a quick arrest of the sample flow. The valves are automatized and software controlled.

C. Sample preparation

Purple membranes (PMs) containing the light-driven proton pump bacteriorhodopsin (bR) as the only protein were prepared from *Halobacterium salinarum* strain S9.[20] PM patches were centrifuged and resuspended in D_2O phosphate buffer (50 mM, pD 7, 150 mM KCl) twice to concentrate the sample into a pellet and to ensure complete H/D exchange. The suspension was adjusted to a final protein concentration of 15 mg/ml and pD 7 with the same buffer. Time-resolved FTIR difference spectroscopic experiments on PM suspension using our UFTIR spectrometer were performed at 23 °C using the IR transparent flow cell described above. For comparison, time-resolved FTIR spectra conducted with the step-scan technique are also shown which were recorded on PM patches immersed in 1M KCl solution in D_2O (pD 6.6). The temperature was 20 °C (see Ref. 21 for details).

D. Results

The performance of the novel spectrometer has been gauged by performing time-resolved experiments on bacteriorhodopsin (bR) employing the ultrarapid scanning capabilities of the spectrometer. bR is considered to be one of the best understood membrane proteins so far[22] and serves as a model system for photosynthesis, ion pumps, and G-protein-coupled receptors. Many biophysical techniques have been developed with research on bR, FT-IR difference spectroscopy being a very prominent example. Since bR is robust and its photocycle is strictly reversible, it is amenable to step-scan experiments, such that the photocycle kinetics have been measured with high time resolution and are well understood. After a short light flash, the molecule switches within picoseconds to the so-called K intermediate. With time constants in the microsecond range, the L and subsequently M intermediate are formed. The N and O intermediates states follow in the range of milliseconds. Several strong bands of the difference spectra between the dark state and the intermediates occur in the mid-IR range between 1800 and 1400 cm^{-1} and document these structural transitions. We limited the spectral range to this region as the IR transmission is strongly attenuated at lower wavenumbers by the solvent D_2O.

Figure 5 shows selected FT-IR difference spectra of the photocycle of bR at different points of time after a laser flash. Purple membranes have been dissolved in D_2O to avoid strong absorption of H_2O in the amide I region. Experiments on PM suspended in excess solvent have been conducted on the novel ultrarapid-scanning spectrometer (Figure 5(a)) and are compared to experiments on purple membrane films which were recorded by step-scan spectroscopy (Figure 5(b), see Ref. 8 for details). Time constants for the reactions of the photocycle depend on several parameters such as pH/pD, temperature, and sample preparation. The absorption changes

in the Fig. 6(a) are 10× smaller than those shown in Fig. 6(b) due to the lower concentration of the protein in solution. The comparison of the step-scan data to the ultrarapid-scanning data shows that the corresponding spectra are in good agreement regarding the intermediate-specific absorption changes. The isomerization of the retinal cofactor is inferred from the C=C stretching vibration which is shifted from 1526 cm^{-1} in the ground state to higher or lower frequencies depending on the respective photocycle intermediate. Changes in secondary structure are derived from the amide I region (C=O stretching vibration of the peptide bond, 1600–1700 cm^{-1}). The difference spectra of purple membranes in solution (Fig. 6(a)) show noticeably stronger changes in the amide I region. It is inferred that structural changes in the protein backbone are larger for the protein dissolved in excess (heavy) water than in a hydrated film as typically used in step-scan experiments. Differences in orientation of the purple membranes in the two samples (uniaxially orientated stacks of PM fragments in the ATR experiments versus isotropically oriented PM fragments suspended in solvent in the transmission experiments) do not account for this observation.[23]

Bands above 1700 cm^{-1} are related to the C=O stretching vibration coupled with the in-plane O–H bending vibration of protonated carboxylic side chains of amino acids. This frequency range is indicative for proton transfer reactions across the protein involving glutamic and aspartic acids.[24,25] A positive band at 1748 cm^{-1} is identified in the difference spectra at 3 ms after the laser pulse (Fig. 6). This band has been assigned to D85[26,27] and appears when this residue accepts the deuteron from the retinal Schiff base. Even the frequency downshift of the C=O stretch of D85 in the later stage of the photocycle is discernible (see difference spectra at 10 ms after photoactivation), again in agreement in both data recordings. After 40 ms, signals have mostly disappeared and the residual difference spectra indicate the noise level in the data.

After the spectral analysis, the kinetics of various marker bands were compared when measured by the two different techniques. Figure 6(a) shows the transient absorption of the band at 1526 cm^{-1} (C=C stretch of retinal) as a function of time. The best fit to these data (continuous red line) was obtained by a sum of three exponentials resulting in time constants of $\tau_1 = 170$ μs, $\tau_2 = 4.5$ ms, and $\tau_3 = 12$ ms. In comparison to the step-scan data recorded on PM immersed in a bulk solution of 1M KCl[9] (plotted in black), the fast and slow time constants τ_1 and τ_3 are a bit faster. This may be due to the lower KCl concentration (i.e. lower surface pD) and the slightly elevated temperature (23 °C in our present experiments as compared to 20 °C in the ATR step-scan experiments[9]).

The kinetic analysis of the deuteration of D85 at 1746 cm^{-1} [28] depicted in Figure 6(b) yielded time constants of $\tau_1 = 610$ μs and $\tau_2 = 12.5$ ms. The data of the immersed film are slowed down as well, in accordance to the C=C retinal band. Both kinetics are very close to what has been previously observed in H_2O.[25]

In summary, it has been shown that the prototype ultrafast FT-IR rapid-scan spectrometer, which is based on the innovative interferometer design presented here, provides high quality data for the elucidation of reaction kinetics. The data of the bR photocycle model reaction reflected band shifts due to H/D exchange and allowed the determination of time constants of sub-processes in the low microsecond regime.

IV. CONCLUSIONS

A novel type of ultrarapid-scanning FT-IR spectrometer with unprecedented temporal resolution has been presented. The prototype spectrometer reported here, has a time resolution of 13 μs at a spectral resolution of 9 cm^{-1}. The ultrafast interferometer comprises an ultrasonic resonator, whose coated front side substitutes the moving mirror in conventional interferometers. The new spectrometer was designed to study fast kinetics of non-cyclic processes, since measurements can be carried out without the condition of a strictly repetitive reaction as it is mandatory for step-scan experiments. Rapid process monitoring and remote sensing over a broad frequency range are made possible in the μs time domain. Moreover, the technique may open new avenues for developments in photoacoustic spectrometry. As the presented spectrometer is three orders of magnitude faster than conventional spectrometers, the thermal wave decay length can be decreased by a factor of 30. In the case of modulated step-scan photoacoustic spectrometry, the modulation of the IR radiation is performed by a moving mirror with an OPD of around 50 μm. This case matches particularly well with the presented invention as small OPDs can be realized at very high frequencies (kHz-MHz), thus facilitating experiments on very thin films.[17]

In combination with recently available high intensity broadband laser sources[29] to replace the globar source, sufficient signal-to-noise of a single 13 μs spectrum will be achieved without averaging. Also, enlarging the surface of the sonotrode mirror will effectively increase the optical throughput Θ (see Eq. (1)) which leads to higher signal-to-noise ratio. To achieve even higher time resolution, stroboscopic sampling[3] may be beneficially combined with the presented spectrometer.

The potential of the invention for the elucidation of fast reaction kinetics has successfully been demonstrated here. Since bacteriorhodopsin is considered to be one of the best-understood membrane proteins and the intermediates of its photocycle have been investigated intensively, it was used as a model system to demonstrate the fidelity of the prototype spectrometer. To emphasize the applicability to non-cyclic processes, experiments were conducted on protein in solution, leading to very small signals. From a technical perspective, the recordings yielded spectra at very high signal to noise ratio. The derived time constants and isotope shifts were comparable to those previously reported. In conclusion, the applicability of the device to protein dynamics in solution has been successfully demonstrated. Experiments in aqueous solution enhance the flexibility of the loop regions of membrane proteins as demonstrated by the larger changes in the amide I mode as compared to the commonly used hydrated films in such experiments.

ACKNOWLEDGMENTS

We thank Tom Resler and Silke Kerruth for help with sample preparation and the group of Ramona Schlesinger (Genetic

Biophysics, Freie Universität Berlin) for the supply of purple membrane fragments. This work has been supported by the Deutsche Forschungsgemeinschaft via SFB-1078, projects A1 and B3.

[1]P. R. Griffith, B. L. Hirsche, and C. J. Manning, Vib. Spectrosc. **19**, 165–176 (1999).
[2]C. J. Manning, U.S. patent 5,898,495 (27 April 1999).
[3]G. D. Smith and R. A. Palmer, *in Time-Resolved Spectroscopy* (John Wiley & Sons Ltd., 2002), p. 625.
[4]A. Rosencwaig, J. Appl. Phys. **47**(1), 64 (1976).
[5]R. M. Dittmar, J. L. Chao, and R. A. Palmer, Appl. Spectrosc. **45**(7), 1104–1110 (1991).
[6]M. R. Alcaraz, A. Schwaighofer, C. Kristament, G. Ramer, M. Brandstetter, H. Goicoechea, and B. Lendl, Anal. Chem. **87**(13), 6980–6987 (2015).
[7]W. Uhmann, A. Becker, C. Taran, and F. Siebert, Appl. Spectrosc. **45**, 390–397 (1991).
[8]C. Zscherp and J. Heberle, J. Phys. Chem. B **101**(49), 10542–10547 (1997).
[9]R. Rammelsberg, B. Hessling, H. Chorongiewski, and K. Gerwert, Appl. Spectrosc. **51**(4), 558–562 (1997).
[10]W. Mäntele, Trends Biochem. Sci. **18**(6), 197–202 (1993).
[11]I. Radu, M. Schleeger, C. Bolwien, and J. Heberle, Photochem. Photobiol. Sci. **8**(11), 1517–1528 (2009).
[12]C. Kötting and K. Gerwert, ChemPhysChem **6**(5), 881–888 (2005).
[13]C. J. Manning, AIP Conf. Proc. **430**(84), 84–95 (1998).
[14]A. Dipal, M. Patel, B. Avadhoot, and U. Rajurkar, in *Nuicone-2011* (Institute of Technology, Nirma University, Ahmedabad, 2011), pp. 1–6.
[15]Fügen von Formteilen und Halbzeugen aus thermoplastischen Kunststoffen mit Ultraschall. (Zentralverband Elektrotechnik- und Elektronikindustrie e.V).
[16]J. W. Brault, Appl. Opt. **35**(16), 2891–2896 (1996).
[17]P. R. Griffiths and J. A. de Haseth, *Fourier Transform Infrared Spectrometry* (John Wiley & Sons, 2007).
[18]T. Hirschfeld, "Quantitative IR: A detailed look at the problems involved," in *Fourier Transform Infrared Spectroscopy: Applications to Chemical Systems* (Academic Press, 1979).
[19]A. K. Atakan, W. E. Blass, and D. E. Jennings, Appl. Spectrosc. **34**, 369 (1980).
[20]D. Oesterhelt and W. Stoeckenius, Methods Enzymol. **31**, 667–678 (1974).
[21]C. Zscherp, R. Schlesinger, J. Tittor, D. Oesterhelt, and J. Heberle, Proc. Natl. Acad. Sci. U. S. A. **96**(10), 5498–5503 (1999).
[22]J. Heberle, Biochim. Biophys. Acta **1458**(1), 135–147 (2000).
[23]J. Heberle and C. Zscherp, Appl. Spectrosc. **50**(5), 588–596 (1996).
[24]M. Engelhard, K. Gerwert, B. Hess, W. Kreutz, and F. Siebert, Biochemistry **24**(2), 400–407 (1985).
[25]J. Heberle, J. Fitter, H. J. Sass, and G. Büldt, Biophys. Chem. **85**(2-3), 229–248 (2000).
[26]M. S. Braiman, T. Mogi, T. Marti, L. J. Stern, H. G. Khorana, and K. J. Rothschild, Biochemistry **27**(23), 8516–8520 (1988).
[27]K. Fahmy, O. Weidlich, M. Engelhard, J. Tittor, D. Oesterhelt, and F. Siebert, Photochem. Photobiol. **56**(6), 1073–1083 (1992).
[28]J. P. Wang and M. A. El-Sayed, J. Phys. Chem. A **104**(18), 4333–4337 (2000).
[29]F. Keilmann and S. Amarie, J. Infrared, Millimeter, Terahertz Waves **33**(5), 479–484 (2012).